A Study of Stress – Induced Subtle Magnetic Changes in a Mild Steel using Barkhausen Emission-Aided Analysis Approaches

A. F. ALTZOUMAILIS[1*], V. N. KYTOPOULOS[2]
[1]School of Chemical Engineering,
National Technical University of Athens,
5 Heroes of Polytechnion Avenue, 15773 Athens,
GREECE

[2]School of Applied Mathematical and Physical Sciences,
National Technical University of Athens,
5 Heroes of Polytechnion Avenue, 157 73 Athens,
GREECE

Abstract: - In this study magnetic Barkhausen emission – based approaches were used to reveal and characterize some interesting elastic stress - induced quantitative and qualitative subtle changes in the micromagnetic activity of steels. The quantitative changes consist in a multiplication of domain walls whereas the qualitative in the formation of two major modes of domain wall motion. Concerning the first kind of changes, it was shown that the experimentally obtained low limit of elastic stress at which such micromagnetic changes may occur is in reasonable agreement with existing theoretical as well as experimental results. Concerning the second kind of changes, it was shown by means of two types of distribution approach, that these two modes of wall motion may be related to the grain boundaries as well as the grain interior micromagnetic activity. In this context, it was also shown that an increase in the supplied elastic strain leads to a broadening of both distribution modes.

1 Introduction

Today, despite extensive and intensive theoretical and experimental investigations, [1], [2], [3], [4], [5], [6], [7], [8], [9], [10], [11], [12], [13], [14], [15], [16], [17], [18], [19], [20], [21], [22], [23], [24], [25], [26], [27], [28], [29], [30], the applied stress – induced micromagnetic effects in ferromagnetic steels are complex and not yet fully understood. In general, the investigation of stress effects on polycrystalline ferromagnetic materials needs a basic reduction to a formulated set of problems solvable by detailed experimental investigations and/or mathematical analysis concerning the dynamics of domain wall motion. As such, the application of stress to material results in a modification of strain state and a corresponding change of its elastic energy, [1], [2], [3], [4], [5], [6], [7], [8], [11], [12], [13], [14], [15] as well as in variations of effective strength levels of domain wall pinning sites, [3], [19]. This is related to the general fact that in ferromagnetic materials, the modification of internal stress – strain results in a change in the free energy and consequent changes in the micromagnetic response of the material, [8], [12], [28]. This leads to an inherent balance between the magnetoelastic and elastic energy of the crystal. In particular, applied stress may modify the energy of domain wall configuration, e.g. the pattern of 180° and 90° domain walls within the grain, [5], [7], [8], [17]. In these materials, position magnetostriction implies that for reasons of energy minimization, domain magnetization should be along the cubic crystal axis that is closest to the direction of applied stress. This results in bulk stress anisotropy, where the direction of the easy axis shifts toward the direction of applied tensile stress, a fact which may be identified with the positive magnetostriction in steel materials, [6], [12], [13]. These results have been associated with certain changes in the relative population of active 180^0 to 90^0 domain walls, where the number of basic domains of 180^0 increases at the expense of supplementary ones of

the 90^0 domain walls, [3], [8]. Moreover, the observed micromagnetic subtle changes have been used to explain for example certain magnetostriction and permeability measurements in dedicated sensor devices, [8], [12], [15]. It should be added that appreciable contribution to the above investigations was given in the early times and the later ones by dedicated visual experimental electron and other microscopic techniques where impressive stress – induced changes in the magnetic domain structure were observed and analyzed, [6], [7], [16], [17], [23].

In this aspect the characterization of stress-dependent micromagnetic properties of steels, for example by Barkhausen emission, is of great importance for the following basic reasons: (i) monitoring applied stresses, (ii) evaluating residual stresses (iii) predicting the signal behavior under conditions of applied stresses and (iv) controlling losses in electrical steels by using stress effective insulation coatings, [8]. As such, Barkhausen emission is a micromagnetic phenomenon that appears as a burst-type signal induced across a coil close to the testing material. This signal is related to the domain wall dynamics and magnetic coupling of the system. As this signal is the manifestation of magnetic noise, its low value often is desirable for many sensor applications. Although the sensitivity of the Magnetic Barkhausen Emission (MBE) to stress is well known, the earlier investigations focused primarily on the overall trends observed as specimens were subjected to deformation, [1], [2], [3], [4], [10], [11], [17], [18], [19], [20], [21], [22], [23], [24], [25], [26], [27], [28]. However, certain inherent anisotropic deformation of crystalline grain may give rise to some subtle changes in MBE at strains far below the elastic limit, [2], [18]. In the context of all the above – mentioned, the present study tried to investigate some of the related processes. In this view, it would be of considerable importance the establishment certain practical and as much as possible simple analysis approaches helpful for a more extended characterization of stress – dependent changes in the micromagnetic response of ferromagnetic materials. In this aspect, these approaches should be described by suitable operational parameters by which the general trend of the related changes can easily be followed and analysed.

2 Material and Method

The chemical composition of the low-carbon steel used in this study is given in Table 1. The used steel had a polycrystalline microstructure with an average grain size of about 30 μ m.

Table1. The chemical composition of used steel

C	Mn	Si	Ni	Cr	Mo	S	P	N
0.05	0.45	0.015	0.015	0.015	0.001	0.018	0.02	0.004

A block diagram of the experimental setup used for measuring the micro-magnetic Barkhausen emission (MBE) parameter is shown in Figure 1. A current from a sweep controller circuit was fed to a bipolar high current generator to generate a symmetric bipolar triangular field. The MBE signal at 10 Hz excitation was acquired by a 2 mm ferrite probe which had 1000 turns and then amplified to 40dB using a low noise amplifier with 10^4-10^5 Hz bandwidth and monitored with a digital oscilloscope using a maximum sampling rate of 100 KHz. It should be pointed out that the utilized sensor of the Barkhausen apparatus was based on a compact type unit described in [30]. In this manner, the accuracy, sensibility, and reliability of the obtained measurements can considerably be improved.
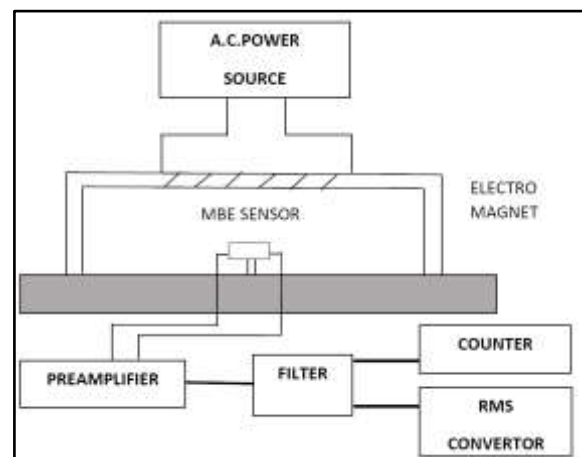

Fig. 1: Block diagram of Micromagnetic Barkhausen Emission setup

The tension test specimens were machined in accordance with ASTM – Method of Tension Testing of metallic materials, E8 – 85 where the thickness was 2 mm and the effective gauge length 100 mm. The specimens were subjected to a room-temperature uniaxial tensile test at a nominal strain rate of 2×10^{-4} sec^{-1}, using a universal INSTRON – type testing machine. The specimens were continuously loaded and data were taken at

convenient time intervals (online measurements). In this sense, each data point plotted on the related curve represents the average value of three measurements. It is noted that when increasing tensile stress is applied to a polycrystal plastic deformation will occur, initially in the most favorable oriented grains. Other grains will not deform beyond the elastic limit region. Thus, the strain distribution becomes non – uniform, with some grains being deformed only elastically and others having local microplastic deformations of the order of $\varepsilon_m = 10^{-4} - 10^{-5}$, [31].

At deformations above the microscopic elastic limit, ε_m, the state of a microscopic continuity is maintained where individual grains are deformed in a matched manner, by retaining continuity on their boundaries. With further increase in the loading, the so-called (upper) yield limit is attained by retaining the macroscopic continuity of polycrystal. For example, in polycrystalline iron, this limit usually corresponds to a deformation of about $2 \times 10^{-4} – 5 \times 10^{-3}$, [31]. Taking into consideration the above statements, we prefer to adopt a conservative microscopic elastic limit $\varepsilon_m = 2 \times 10^{-4}$ for our related loading program.

To conduct the desired pulse (count) energy discrimination measurements, the Barkhausen instrumentation was used as follows: The counter module of the apparatus is set to work as an energy discriminator or screening factor. As such, it is used to select and transmit the counts (pulses) within a predetermined voltage range for further processing. Practically this is achieved by selecting variable sets of threshold baseline voltage or discrimination energy levels. In other words, the emitted Barkhausen events (pulses) of energy lower than the predetermined energy level are rejected whereas pulses at higher energy levels are accepted and processed by the apparatus. In this way, by stepwise increase, (decrease) of the threshold voltage level and measuring the number of accepted counts (pulses), it is possible to obtain a certain valuable energy-type distribution of the total emitted Barkhausen signal and consequently to get a complementary insight into the (elastic) stress – controlled micromagnetic activity in the material. The above-mentioned instrumental setting is referred to as integral in contrast to the differential one where the operator by means of potentiometer controls may set a combination either of a baseline voltage and a window voltage or of a baseline and an upper window voltage. In all cases the proper setting of the discriminator is crucial because if it is too low, the noise will be accepted as pulses, however, if it is too high, low –

energy pulses might be missed. Pileup rejection is therefore more complicated for low – energy pulses which may be hard to separate from the background noise.
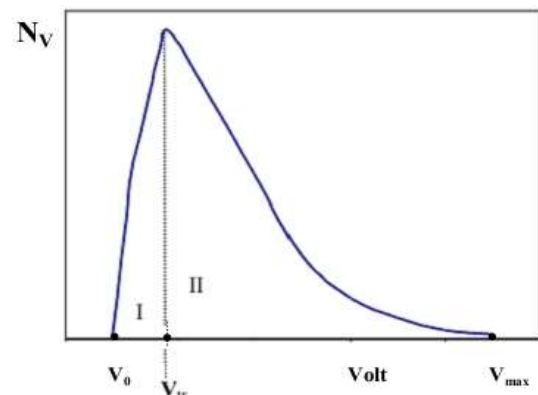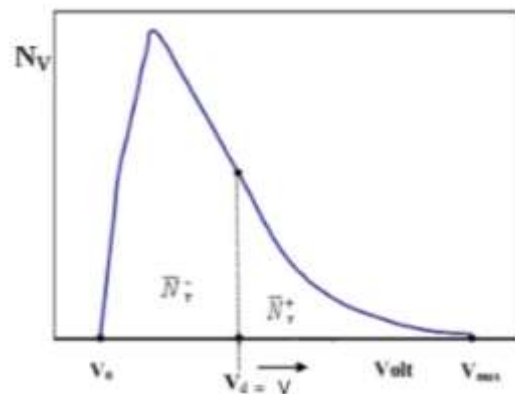

Fig. 2: Sketch of a common PHD

Fig. 2a: Sketch of the generation of an integrated PHD. (arrow indicates the direction of applied discrimination Voltage, $V_d = V_{tr} = V$).

3 Theoretical *Considerations*

The sketch shown in Figure 2 simulates a common pulse height distribution, (PHD). Thus, by making a working premise, one can tacitly assume that this distribution should arise from a total overlapping of two different PHDs, each one expressing an associated different kind of micromagnetic activity: grain boundary and grain interior activity, [22], [23]. This total overlapping might be probably attributed to the reduced sensitivity or resolution power of the common PHD – technique to produce a sufficient separation of peak positions of each distribution to show up in the PHD profile. The reduced sensitivity could be substantiated by the following facts. As shown in the sketch, the pulses (counts) are detected above a certain finite "dead" voltage V_0, although in reality, a non-vanishing magnetic activity should exist for limiting voltages

$V \rightarrow 0$. This in turn is supported by the fact that applied stress can create wall motion and hence a finite signal without the application of a magnetic field, [19]. The "missing" pulses below the "dead" voltage, in our opinion, can be attributed to the background electronic noise of the detecting circuit, which may suppress these pulses. As such, this "dead" voltage could exist, among others due to thermal fluctuation – induced background noise effects, indicative of the anticipated reduced sensitivity of the common PHD – technique. In this aspect magnetization frequency, time response of pick-up coil, and deat time of electronic system may also contribute to reduced detection sensitivity. At this place, it should further be explained that pulse suspression- may occur, among others, as an inherent "weakness" of the electronic system to distinct between two pile – upped pulses. Pulse pile-up is an inevitable phenomenon and may occur when a pulse arrives at the detector before the linear amplifier has finished processing the preceding pulse. It appears as an increased output pulse height for the second pulse because it is riding on the tail of the first. Pulse pileup can also appear as a single large pulse representing the combined voltages of two pulses if the second pulse arrives before the pulse from the first has reached its maximum value. Thus, in the most extreme case, two pulses may arrive at the detector almost simultaneously, and the output becomes a single combined pulse corresponding to the sum of two pulse energies. In particular, pulse, pile – up operation is more complicated for low – energy pulses which may be hard to separate from the background noise. Nevertheless, pulse, pile up can be reduced by decreasing for example the processing time for each pulse, since shorter linear – amplifier output pulses are less likely to interfere with each other. This is accomplished electronically through user selection of the linear – amplifier time constant (T.C.), which determined the output pulse width. However, the T.C. can only be an indication of the pulse width, since the acceptable time between pulses may be many times the value of the selected T.C. From the above-described pulse suppression one can argue that this may contribute to the reduced sensitivity of the electronic system.

It was stated that the peculiarity of grain boundary region, due to its microstructural character and geometry as well as its configuration such as inclinations and connectivity, may result in a related peculiar transition of micromagnetic activity from switching of static domain walls to varying jumping displacements of domain walls moving from and / or towards grain boundary, [8], [22], [28]. Due to this peculiarity magnetic domains in the vicinity of grain boundaries are affected more differently than those in the grain interior regions, [22], [23]. On the other hand, domain wall jumps taking place within grain interior regions may sweep out the large volume for short time giving rise to an induced voltage of large amplitude. Therefore, from Figure 2 one can presume that low – voltage region I, might express the grain boundary – controlled domain wall motion whereas the high – voltage region II, the grain interior – controlled wall motion, [22], [23]. Consequently, the V_{tr} voltage value corresponding to the maximum (pick) of distribution in Figure 2 could be seen to represent the transition point between the two regions. Furthermore, in the sketch of Figure.2a the essential principle of the adopted integrated PHD method is depicted.

Hence, taking into consideration the measurement procedure presented in the Experimental Section, the left side area, extended from V_0 to variable discrimination voltage $V = V_d$ represents the rejected – not measured average number of pulses (counts) denoted by $\overline{N_V^-}$. On the other hand, the right side area, extended from variable V_d to maximum voltage V_{max} which is the limiting voltage where a vanishing number of counts are detected, represents the accepted – measured pulses (counts) demoted by $\overline{N_V^+}$.

More explicitly, the following general relationships hold

$$\overline{N_v^-} = \int_{V_0}^{V_d} N_v dV; \quad N_v^+ = \int_{V_0}^{V_{max}} N_v dV$$

With $\quad \overline{N_v^-} + \overline{N_v^+} = \overline{N_v^{tot}} = \quad \int_{V_0}^{V_{max}} N_V dV =$ total average number of measured counts.

In this aspect, the adopted measurement technique turns out practically to be an integrated pulse height distribution approach, where the data, by variation of the threshold – discriminating voltage V_d, are obtained as a result of a stepwise integration procedure of the common PHD – curve.

By this integration two main advantages arise compared to the common PHD – procedure; first: small, undesirable statistical variation of measurements observed in the common PHD-curve is in a great part averaged out; second: in this way at the same time, valuable differences produced between common PHD-curves are enhanced for a more easy data analysis. In this context we believe, generally speaking, that the advantages of the used

integration procedure arise 'ultimately' because of the inherent dependence of the common PHD-procedure on the proper setting of the window size

4 Results and Discussion

4.1 General Aspects

In Figure 3 the evolution of the measured counts versus applied elastic strain (stress) for certain predetermined increasing threshold discriminating voltage levels $V_{i+1} > V_i$ $i = 1,2,......6$ in steps of 0.1 Volt is presented. Thus, in this Figure, the low energy transitions V_1, V2, and V3 are enhanced whereas the higher energy transitions V_4, V5, and V6 are depressed.
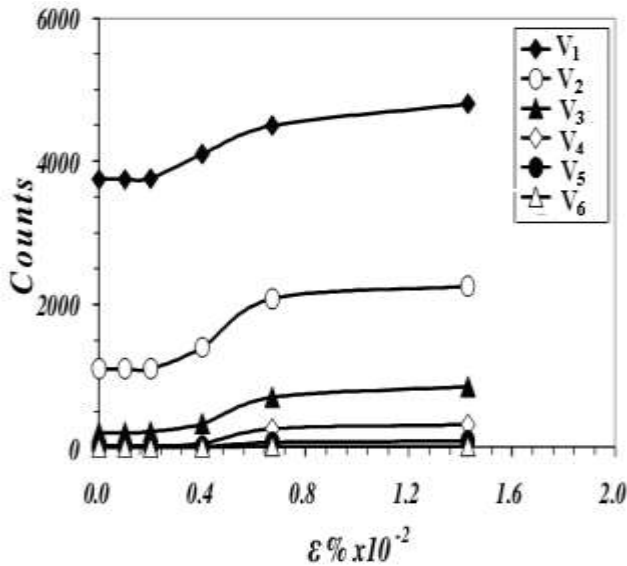

Fig. 3: Evolution of measured counts versus applied elastic strain for six predetermined values of threshold voltage levels
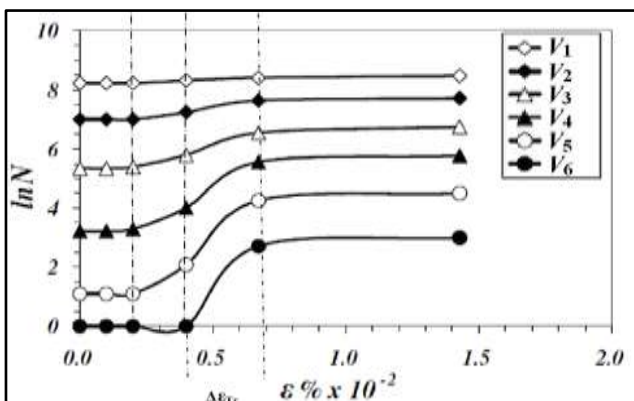

Fig. 3a: logarithmic mode of counts evolution versus applied elastic strain for six predetermined threshold voltage levels

In Figure 3a the evolution of the logarithmic, $ln(N)$, number of counts versus strain for the same six predetermined increasing threshold voltage sets $V_{i+1} > V_i$, $i = 1,2,......6$, in steps of 0.1 Volt is shown. By this mode of presentation, a more clear transition range of these evolutions can be revealed. As such, in Figure 3a the opposite trend is observed in the sense that high energy transition levels V4, V5, and V6 are enhanced, while low energy transitions V_1, V2, and V3 are depressed. The above modes of presentation allow also us to observe that at a certain critical strain (stress) an increase in the number of counts occurs, resulting in a transition stress (strain) range of the magnetic activity from 10 MPa or 4×10^{-5} strain to 18 Mpa or 7.0×10^{-5} Strain. This gives an average transition stress of about 14 MPa. A reasonable explanation of the above transition behavior might be given for example by the mechanisms proposed in [3], where an increase in the 180^0 domain walls population with applied elastic tensile stress may occur.

However, in the cited study a theoretical minimum elastic stress level of about 32 MPa was calculated by these mechanisms. This value is larger than that obtained in the present experimental study. Nevertheless, our approximating calculation made with respect to the cited study, showed that by taking into consideration certain parameters of the present material, this "critical" level could be reduced to about 18 MPa. It is worth noting that similarly low critical elastic stresses of about 10 MPa were observed for activation of wall multiplication phenomena by means of the stress coatings technique, [8], where these phenomena were related to the fact that tensile stresses suppress the supplementary – transverse domains resulting in a decrease in the basic domain spacing and hence an increase in the measured count rate. As regards these phenomena, impressive detailed low stress – induced domain wall multiplications and annihilation processes were observed in iron and extensively discussed in early and recent excellent experimental monographs, [8], [16], [17].

4.2 Energetic Distribution

In Figure 4 the evolution of measured counts (pulses) versus squared applied discrimination voltage is presented. For a better and more convenient interpretation of the data, this exponential – type of evolution indicates to adopt in a first approximation a natural logarithmic mode of presentation. Therefore, in Figure 5, the evolution of this natural logarithmic number of

detected counts versus squared threshold voltage, V^2, for given elastic tensile strain (stresses) is presented.
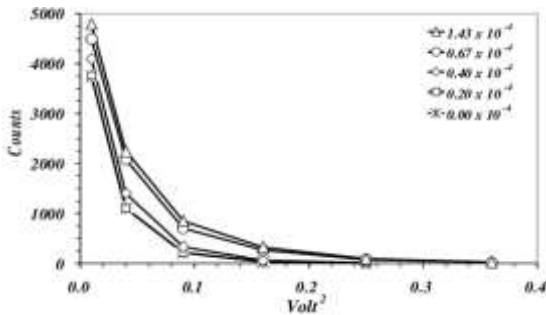

Fig. 4: Distribution of measured counts versus squared levels for given values of applied elastic strain.
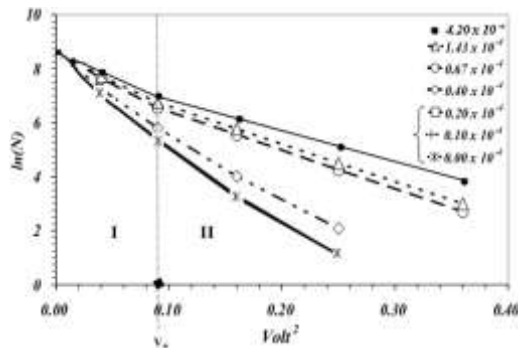

Fig. 5: Natural Logarithmic mode of count distribution versus squared threshold voltage levels for given values of applied elastic strain.

As such, within the limits of experimental scatter, the interesting formation of two major, quasi – linear regions I and II, separated by a "smeared" transitional point V_{tr} can reasonably be distinguished. To avoid any degradation of the distinctness of the curves in Figure 5, the data corresponding to zero, 0.1×10^{-4} and 0.2×10^{-4} strains are plotted together as an initial state by a single point because these data almost coincide. The observed quasi "linearity" of these regions suggests adopting an exponential energetic distribution behavior of the emitted counts. Starting from the fact that the induced voltage, in a first approximation, should be proportional to the average wall velocity, [25], the following relationship should hold:

$$(\text{Volt})^2 = V^2 \approx \bar{V}_W^2 =$$
$$(\text{Average wall velocity})^2 \propto (\text{Wall kinetic energy}) =$$
$$E_W = \frac{1}{2}\text{m} \cdot \bar{V}_W^2,$$

where m denotes the effective Döring inertial wall mass, [8]. Hence, trying to introduce a distribution approach one can further proceed formally as follows:

$$\bar{N} = N_0 \exp\left(-\tilde{\beta} \cdot \frac{1}{2}\text{m} \cdot \bar{V}_W^2\right) = N_0 \exp\left(-\tilde{\beta} \cdot E_W\right) = N_0 \exp\left(\frac{-E_W}{E*_w}\right),$$

where $\bar{N}$ is the average number of measured counts, N_0 a count amplitude, and

$$E*_w = \frac{1}{\tilde{\beta}}, \quad \text{where } \tilde{\beta} \text{ is an exponential energetic}$$

accommodation constant. As such, henceforth $E*_w$ is denoted as a characteristic energy scatter number which describes the distribution broadening (narrowing) behavior.

It must be noted, that the effective inertial wall mass (m) in the above equations is assumed to be an averaged - constant parameter since mass differentiation or variation effects caused by possible wall clustering phenomena could reasonably be neglected. This is because a relatively high magnetizing frequency (10Hz) is used in the present study, allowing so respective short correlation time between elemental pulses (transitions) and hence a reduced clustering effect. In general, it can be shown that when the magnetizing frequency increases or the sample becomes thicker, as in the case of the present study, the clustered nature tends to vanish, [25]. Furthermore, it was also shown that elastic stresses compared to stresses in the plastic regime should lead to a reduced clustering tendency, [25]. Now, by taking into consideration the above explanation and Fig. 5, one may derive the following formulas concerning the two distribution regions I and II:

$$\bar{N}_I = N_0 \exp\left(\frac{-E_W}{E*_{W,I}}\right) \tag{1}$$

$$\bar{N}_{II} = N_0 \exp\left(\frac{-E_W}{E*_{W,II}}\right) \tag{2}$$

Where $\bar{N} = \bar{N}_I + \bar{N}_{II}$.

Furthermore, after a linear transformation one can obtain

$$ln\bar{N}_I = \frac{-E_W}{E*_{W,I}} + ln N_0 \tag{1a}$$

$$ln\bar{N}_{II} = \frac{-E_W}{E*_{W,II}} + ln N_0 \tag{2b}$$

Thereafter, for the individual regions I and II, one can set

$$E^*_{W,I,II} = + \frac{1}{a_{I,II}} \qquad (3a)$$

Where $a_{I,II}$ is the slope of the linear equations (1a) and (2b).

This means that the characteristic energetic scatter number reflects the inverse of the slope of the linear regions. In this way, one would obtain an operational measure of the magnetic activity changes. For instance, as it can be estimated from Figure 5, an application of elastic stress (strain) of about 29 MPa (1.43 10^{-4}), leads to a noticeable increase of about 30% in the characteristic scatter numbers $E^*_{W,I,II}$ compared to the initial state. Consequently, one can reasonably state that an increase in the applied strain energy results in a corresponding broadening of the respective energetic distribution of the moving domain walls. Thereafter, a plausible explanation of the mentioned general increase in the characteristic scatter numbers of both regions could be given as follows: an application of stress leads to an inhomogeneous variation in the pinning strength, and in many cases, this fact results in a premature breaking away of the domain walls from their pinning sites, [3], [19]. These facts encourage an increased variation of associated wall velocities, resulting in a broadening of their distribution and hence an increase of characteristic energetic scatter number. It seems, in general, that the combined effect of an increase in the wall population and a broadening of pinning strength distribution may stimulate a broadening of the wall velocity or energetic distribution reflected by an increase in the characteristic energy scatter numbers $E^*_{W,I}$ $E^*_{W,II}$.

Furthermore, if we pay attention to Figure 5, should focus on the increased difference created between the distribution for 0.4 x 10^{-4} and 0.67 x 10^{-4} strain in the sense that this corresponds to the largest one created between consecutive strains. One could assume that within this strain range, certain 'critical, 'elastic anisotropy induced micromagnetic processes may occur resulting in an enhanced broadening of distribution. Moreover, for higher applied elastic strains of 4.2 10^{-4} a further small change in the distribution occurs. This can be related to the fact that for a strain larger than the earlier adopted microscopic elastic limit 2x10 $^{-4}$, certain localized microplastic deformation, in form of dislocation multiplications and formation of dislocation pile - ups at grain boundaries, may take place resulting in a more or less inhomogeneous

pinning sites density and therefore in a further broadening of distribution. At the same time, for certain elastic strains (stresses), the quasilinearity of the two regions, separated by V_{tr}, seems to be improved, indicative of the different micromagnetic response of these regions. This is because for these strains intensive elastic accommodation processes at grain boundaries may take place, [22], [31] by which their micromagnetic contribution to the total one is enhanced.

At this place, it should be noted that similar two quasi- linear distribution ranges were obtained by the authors in their ongoing investigation for deformations beyond the yield point. However, with increasing plastic strain both regions seem to merge into a single non-linear region. This could be due to the fact that with plastic deformation the dislocation density increases rapidly and becomes more homogeneous. In this instance, the magnetic microstructure is dominated by associated relative homogeneous pinning site density. As such, dislocation pileup - in duced long-range stress fields tends to "smear" the individual contribution of the grain boundary and grain interior region to the total micromagnetic activity.

Furthermore, as it was shown earlier, by means of the observed slopes of each quasi-linear regions I and II, it can be argued that $E^*_{W,I} < E^*_{W,II}$. , This energetic scatter inequality is an interesting finding which allows the possibility of a co – existence of two corresponding distinctive wall motion modes I and II. In other words, the above inequality means that the wall motion mode I is connected to a lower characteristic energetic scatter compared to mode II.

A plausible interpretation of these findings could be given as follows:

High pinning sites density and strength at grain boundaries caused by several processes such as crystal lattice distortion, elastic grain boundary accommodation, dislocation accumulation, precipitations as well as grain misorientation – induced stray fields, and magnetic closure domains, force the domain walls to move by small jumping and rotation steps with reduced velocity within short time periods, [22], [23]. On the other hand, in the grain interior, due to lower pinning sites density and strength, the walls can move almost freely, within larger time periods, over longer distances, attaining associated larger jumping steps and higher velocity. Thus, it could be argued that small time periods of micromagnetic activity may allow a reduced probability of the wall velocity and hence the wall energy to change considerably from its

mean value, while large time periods should favor such a probability. From the above arguments, it can reasonably be assumed that the formed region I in Figure 5 might be related to the wall motion within the grain boundary i.e. to a low mobility transcrystalline mode, whereas formed region II to the wall motion within grain interior, i.e. to a high mobility intracrystalline mode.

4.3 Impulse–angular Momentum Distribution Mode

The graph of this mode is given in Figure 6 where the natural logarithmus of the number of measured counts is plotted versus applied discrimination voltage. In this aspect, the approach to an impulse / angular momentum distribution can formally be obtained as follows:

Impulse = I= $\int_0^t F_d \mathrm{dt} = p - p_0 = m\overline{V_w} - m\overline{V_0}$, where t is the flying or displacement time of domain walls, F_d the driving force and $\overline{V_w}$ is the average wall speed proportional to the applied threshold voltage. Yet, $\overline{V_0} = 0$ at time t=0 of pinning instant.
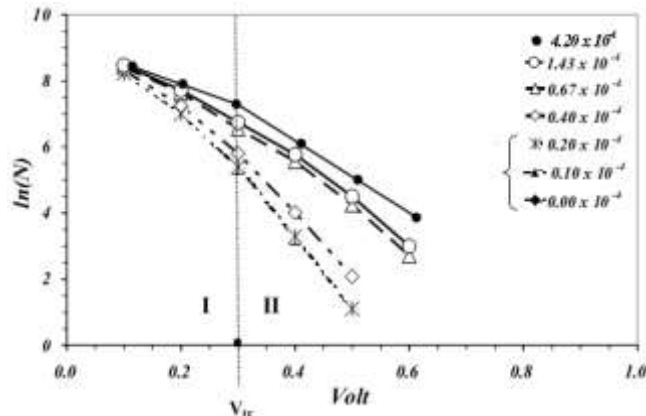

Fig. 6: Natural Logarithmic mode of count distribution versus threshold voltage levels for given values of applied elastic strain.

Furthermore, angular momentum = L = $\int_0^t \tau \mathrm{dt}$ is given where τ denotes the torque of driving force $\tau = |\vec{r} \times \vec{F_d}| = r \cdot F_d \cdot \sin\psi$, t is the rotation time of pinned domains, r = effective domain length, and ψ the angle between driving force and domain length axis.

Thereafter, one obtains: $L = \int_0^t \int_0^{\pi/2} r \cdot F_d \cdot \sin\psi d\psi \mathrm{dt} = r\overline{\sin\psi} \int_0^t F_d \mathrm{dt} = c \cdot I$, with $\overline{\sin\psi} = \frac{2}{3}$

(6)

and $c = \frac{2}{3} r =$ constant.

By this equation, the angular momentum mode of presentation becomes equivalent to the impulse mode.

Thereafter, similarly to the earlier presented energetic distribution procedure, one can formally introduce $I^*_{I,II} = \int_0^t F_d dt$, as a characteristic impulse scatter number for the corresponding quasi-linear regions I and II of the distribution shown in Fig. 6. Taking further into consideration a similar behavior of energetic distribution as given by eqs (1) and (2), one can assume that $I^{*b}_I > I^{*\mathrm{int}}_{I,II}$. This means that the grain boundary – controlled impulse scattered number should be larger than the grain interior scatter number. A first plausible explanation could be given as follows: In the impulse mode both driving force and time of domain response are simultaneously subjected to comparable variations due to interactions with crystal lattice defects. Thus, in the grain boundary regions strong crystal lattice distortions prevail, leading to large impulse variations connected with large time scatter t *, a fact caused by high pinning strength – induced accelerated and/or decelerated wall motion. Consequently, the response time determined by domain flying and / or rotation time may markedly vary by giving a large time scatter. This means in other words that this scatter may become very sensitive to interaction effects due to pinning strength variations induced - by acceleration and /or deceleration effects of the moving walls. Moreover, as in the case of the energetic distribution approach, one can observe from Figure (6), that an increase in an applied elastic strain leads to an increase in the impulse scatter number and therefore to a broadening of the impulse distribution. This is because, as earlier mentioned, stress – induced inhomogeneous pinning strength variations and elastic grain boundary accommodation processes may stimulate such a broadening of this distribution.

Last but not least, the presented findings of a possible co – existence of two major types of micromagnetic activity could be considered to have an equivalent meaning with the findings presented in [22], where due to the peculiarity of the microstructural character of the grain boundary regions, the measured Barkhausen signal follows a Hall – Petch – type dependence on grain sizes. In this aspect, the present findings could be indicative of the capability of the proposed analysis approaches to discriminate between grain interior and grain boundary regions making these

approaches a convenient and reliable tool for further similar investigations.

5 Conclusions

From the present investigation, the following essential conclusions can be extracted:

➢ Elastic stress (strain), applied far below the macroscopic elastic limit, may facilitate subtle quantitative as well as qualitative changes in the micromagnetic activity of ferromagnetic steels. The first ones are characterized by an increased number of domain walls, whereas the second is by the formation of two major modes of domain wall motion.

➢ The obtained quantitative findings concerning the threshold characteristic stresses at which such subtle micromagnetic changes may occur are in reasonable agreement with the existing theoretical and experimental results.

➢ By means of two kinds of operational distribution approaches, the possibility of the (co) – existence of two major characteristic wall motion modes can reasonably be demonstrated: a transcrystalline one, related to grain boundary and an intracrystalline one, related to the grain interior region.

➢ An increase in the supplied elastic energy results in a broadening of the distributions, a fact that can primarily be attributed to certain mechanisms of stress – induced inhomogeneous variations of the pinning strength barriers, and secondarily to elastic grain boundary accommodation processes.

➢ Based on measurements made by an integrated magnetic Barkhausen pulse height distribution technique, the introduced analysis approach, as a complementary one, seems to be a reliable, and convenient tool helpful for a further similar investigation to get valuable information regarding the physical and mechanical characterization of applied - elastic stress – coupled micromagnetic changes in steels.

References:

[1] Mohamad Blow, J.T. Evans and B. A. Shaw, J. Mat. Sci. Vol. 42, (2007) pp 4364 – 4371

[2] C. G. Stefanita, L. Clapham and D. L. Atherton, J. Mat. Sci., vol.35, (2000) pp. 2675-2681

[3] T. W. Krause, L. Clapham, A. Pattantyus and D. L. Atherton, J. Appl. Phys., vol. 79(8), (1996) p. 4242

[4] C. G. Stefanita, D.L. Atherton, and L.Clapham. J. Acta Mater. 2000, 48(13), pp3545-51.

[5] C. Jagadish, L. Clapham and D. L. Atherton, J. Phys. D: Appl. Phys., Vol 23, (1990), pp. 443-448.

[6] J. W. Shilling, J. Appl. Phys. Vol. 42(4), (1971), pp. 1787-1789

[7] L.J. Dijkstra and U.M. Martius, Reviews of Modern Physics Vol. 25, (1953) No. 1 pp 146 - 150

[8] Alex Hubert and Rudolf Schafer (2000) "Magnetic Domains: The analysis of Magnetic microstructures", Springer Verlag, Berlin, Heidelberg, New York

[9] R. M. Bozorth, (1951) Ferromagnetism, Van Nostrant, Princeton.

[10] E.K.Ioakeimidis, V.N.Kytopoulos and E. Hristoforou (2013) Mat. Sci. Eng. A, Vol.583, pp254-260, (2013).

[11] Mohamad Blow, J.T. Evans and B. A. Shaw (2004) Mat. Sci. Eng. A, Vol. 386, (2004) pp 74 – 80

[12] Martha Pardavi – Horvath (1999) Magnetic Noise, Barkhausen Effect, in Wiley Encyclopedia of Electrical and Electronic Engineering J. E. Webster Ed. 12:52-64.

[13] Jagadish C., Clapham L., Atherton D.L., (1990) IEEE Trans. Magn., 26: 1160

[14] Sablik M.J., Augustyniak B., J. in Wiley Encyclopaedia of Electrical and Electronic Engineering 12: 24 – 26, J. E. Webster Ed.

[15] E. Hristoforou., P. Vourna, A. Ktena, P. Svec, (2016) IEEE Transactions on Magnetics, 52:7362189.

[16] L.W. Kirenskij (1969) Magnetismus (in German), Leipzig BSB, B.E. Teubner Verlagsgesellschaft.

[17] D. E. Newbury, H. Yakowitz (1976) Practical Scanning Electron Microscopy» Chapter VI Plenum Press, N.Y. and London J. I. Goldstein and H. Yakowitz, Eds.

[18] V. N. Kytopoulos, E. K. Ioakeimidis (2014) Key Engineering Materials 605: 637-640.

[19] D.C. Jiles and D.L. Allerton (1984) J. Phys. D 17: 1265 – 1281.

[20] M. Lindgren, and T. Lepisto (2001) NDTgE International, 34:337-344.

[21] A. Dhar, L.Clapham, D.L.Atherton (2001) NDTgE International, 34:507-514.

[22] Yamaura S., Furuya Y., Watanabe T (2001). Acta Mater, 49:3019-3027

[23] Jia Liu, Fasheng Qiu, Gui Yun Tian and Bin Gao, (2018) J.Magn, Magn.Mater, 471

[24] Tiitto SI(1978) IEEE Trans. Magn. 14 :527

[25] D. E. Hwang and H. C. Kim (1988) J. Phys. D.: Appl. Phys. 21: 1807 – 1813.

[26] Tiito S. and Saynajakangas S (1975) IEEE, Transactions on Magnetics, 11(6).

[27] Kypris O., Nlebedim I.C. and D.C. Jiles (2014) Appl.phys 115:1-5.

[28] N.Kasai, H. Koshino, K. Sekine, H. Kihira and M. Takahashi (2013) J.Nondestructive Eval.32 (3):.277- 285.

[29] Yonka Ivanova (2018) MATEC Web of Conferences 145, 05007NCTAM.

[30] J. Grum, B. Pecnikint. (2006) J. of Materials and Product Technology.26 (1/2):152- 162.

[31] P. Polukhin, S. Gorelik, V. Vorontsov (1982) Physical principles of plastic deformation. Mir Publisher [in English].

Contribution of Individual Authors to the Creation of a Scientific Article (Ghostwriting Policy)
The authors equally contributed in the present research, at all stages from the formulation of the problem to the final findings and solution.

Conflict of Interest
The authors have no conflict of interest to declare that is relevant to the content of this article.